Materials Research Letters

ISSN: (Print) 2166-3831 (Online) Journal homepage: https://www.tandfonline.com/loi/tmrl20

Excellent superelasticity in a Co-Ni-Ga high-temperature shape memory alloy processed by directed energy deposition

C. Lauhoff, N. Sommer, M. Vollmer, G. Mienert, P. Krooß, S. Böhm & T. Niendorf

To cite this article: C. Lauhoff, N. Sommer, M. Vollmer, G. Mienert, P. Krooß, S. Böhm & T. Niendorf (2020) Excellent superelasticity in a Co-Ni-Ga high-temperature shape memory alloy processed by directed energy deposition, Materials Research Letters, 8:8, 314-320, DOI: 10.1080/21663831.2020.1756495

To link to this article: https://doi.org/10.1080/21663831.2020.1756495

Published online: 30 Apr 2020.

MATER. RES. LETT.
2020, VOL. 8, NO. 8, 314–320
https://doi.org/10.1080/21663831.2020.1756495

MATERIALS RESEARCH LETTERS
Taylor & Francis
Taylor & Francis Group

ORIGINAL REPORT

Excellent superelasticity in a Co-Ni-Ga high-temperature shape memory alloy processed by directed energy deposition

C. Lauhoff[a], N. Sommer [b], M. Vollmer [a], G. Mienert[b], P. Krooß [a], S. Böhm[b] and T. Niendorf [a]

[a]Institute of Materials Engineering, University of Kassel, Kassel, Germany; [b]Institute for Production Technologies and Logistics, University of Kassel, Kassel, Germany

ABSTRACT

A Co-Ni-Ga high-temperature shape memory alloy has been additively manufactured by directed energy deposition. Due to the highly anisotropic microstructure, i.e. columnar grains featuring a strong near-⟨001⟩ texture in build direction, the as-built material is characterized by a very low degree of constraints and, thus, shows excellent superelasticity without conducting a post-process heat treatment. As characterized by *in situ* deformation testing and *post-mortem* microstructural analysis, additive manufacturing employing directed energy deposition seems to be highly promising for processing of shape memory alloys, which often suffer difficult workability.

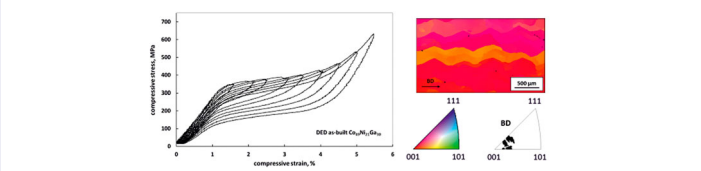

IMPACT STATEMENT

The present work establishes a new pathway towards realization of high performance shape memory alloys by additive manufacturing and, thus, will stimulate further research in this field directed towards application.

ARTICLE HISTORY
Received 6 March 2020

KEYWORDS
High-temperature shape memory alloys; additive manufacturing; laser melting; pseudoelasticity; direct microstructure design

Introduction

In recent decades high-temperature shape memory alloys (HT-SMAs) featuring increased martensite start temperatures (M_s) have been designed to operate at temperatures above 100°C [1]. This is necessary, since the inherent application temperature limit of near equiatomic binary Ni-Ti hinders its technological breakthrough in high-temperature applications, e.g. in the fields of aerospace, automotive, and the energy sector [1,2]. Numerous alloy systems have been developed and proposed so far. Up to now, ternary Ni-Ti-Hf is the most promising HT-SMA, since substantial progress has been made recently with respect to processing and functional performance [3,4]. Still, costs are quite high due to the high amounts of Hafnium [1].

Among the alternative candidate systems, the Heusler-type Co-Ni-Ga alloys undergoing a martensitic transformation (MT) from B2-ordered austenite to $L1_0$ martensite [5] have received increasing attention [6]. In single-crystalline state, Co-Ni-Ga shows excellent functional performance at elevated temperatures, i.e. a fully reversible superelastic (SE) response up to 500°C and excellent cyclic stability up to 100°C [7–9]. Moreover, a recently introduced design concept based on aging of stress-induced martensite, referred to as *SIM-aging* [10], enables direct tailoring of the transformation temperatures. Thus, in addition to the promising high-temperature damping properties, Co-Ni-Ga can be qualified for high-temperature actuation as well [10,11].

Unfortunately, polycrystalline material suffers premature failure, i.e. particularly intergranular cracking upon thermo-mechanical loading and/or processing [1,12,13]. In microstructures without preferred grain orientation, the pronounced anisotropy of the transformation behavior [14] results in incompatibilities at grain boundaries (GBs) between grains of different crystallographic orientations. These incompatibilities cannot be sufficiently accommodated during MT and, thus, grain constraints

CONTACT C. Lauhoff lauhoff@uni-kassel.de Institute of Materials Engineering, University of Kassel, Kassel 34125, Germany

lead to early fracture [1]. A key criterion for enhanced functional properties in relatively brittle and anisotropic SMAs, such as Cu- and Fe-based SMAs and Co-Ni-Ga, is a microstructure avoiding grain constraints [15,16]. Ueland and Schuh [16] identified large GB areas and, particularly, GB triple junctions as the most detrimental microstructural features evoking stress concentrations and eventually rapid structural and functional degradation. In line with those findings, Liu et al. [17] found excellent SE in continuous unidirectional solidified Cu-Al-Mn SMA featuring solely columnar grains with a strong ⟨001⟩ texture and absolutely straight GBs of low-angle character. Another approach aims at realization of oligocrystals, i.e. so-called bamboo structures, being characterized by a minimized GB area and the absence of triple junctions [15,18]. Recently, a novel thermo-mechanical processing route based on hot extrusion followed by a post-processing heat treatment has been introduced to obtain bamboo structures and enhanced shape memory properties in polycrystalline Co-Ni-Ga [19,20]. However, processing remains highly challenging and, thus, alternative process routes for designing adequate polycrystalline SMA microstructures, being able to withstand grain boundary induced collapse, have to be identified.

In recent years, additive manufacturing (AM) has gained lots of attention as a technology allowing for direct microstructural design [21,22]. In numerous AM processes, solid metallic components are fabricated directly from a computer-aided design (CAD) file by melting successive layers of a metallic feedstock material using a focused laser or electron beam. During processing, the solidification mode and the resulting microstructural features, i.e. texture and grain morphology, are dependent on the thermal gradient and the solidification velocity [23]. By adequate control of the process-related parameters, tailored microstructural features have been obtained in various materials [21,24]. In consequence, alloy-specific microstructural design seems to be highly promising to provide for enhanced functional material properties in anisotropic SMAs. In a very recent study, the present authors processed Co-Ni-Ga HT-SMA via powder-bed based selective laser melting (SLM) technique [25]. Using this technique, a columnar-grained microstructure evolved. However, data focusing on the functional properties of additively processed Co-Ni-Ga have not been reported so far.

The current study focuses on the SE properties of samples processed by the powder-stream based directed energy deposition (DED) technique. *In situ* incremental strains tests (ISTs) accompanied by optical microscopy (OM) and *post-mortem* scanning electron microscopy (SEM) analysis using electron backscatter diffraction (EBSD) technique were conducted and used to establish the relationship between the excellent functional properties and the highly anisotropic microstructure obtained for DED processed Co-Ni-Ga SMAs.

Material and methods

In this study a $Co_{49}Ni_{21}Ga_{30}$ (in at.%) HT-SMA was additively manufactured by DED. The chemical composition is designed for enhanced functional properties characterized by a high degree of strain recoverability [7]. Co-Ni-Ga powder was obtained by gas atomization of as-cast material (TLS Technik, Bitterfeld, Germany). The chemical composition of the initial as-cast material was 48.9 Co, 21.0 Ni and 30.1 Ga (in at.%) as determined by X-ray fluorescence analysis (XRF). Chemical composition of the powder material was double-checked using energy-dispersive X-ray spectroscopy (EDS). For fabrication a 2 kW multi-mode fiber-laser with a wavelength of about 1070 nm operating at 400 W was used. The laser optics were mounted to a six-axis robot. The traverse speed was set to 10 mm s^{-1}. Powder material with an average particle size < 20 µm and spherical shape was fed with a rate of 16.8 g min^{-1} to a three-jet-nozzle using a two-channel powder feeder and argon carrier gas. Cuboid blocks with dimensions of 40*30*3.5 mm^3 were built on Co-Ni-Ga substrate material, which was aligned to a preheated baseplate. The baseplate temperature was continuously kept at 500°C throughout the entire build process. In order to avoid contamination, argon was used as shielding gas during processing. Only a slight change in chemical composition (the Ga content of the as-built material is decreased by about 0.5 at.%) was determined by EDS as a result of the DED processing. 180° alternating scanning directions between successive layers were employed resulting in a quasi bidirectional scanning strategy. Individual tracks were deposited in each layer with an overlap of 0.7 mm.

Compression samples with dimensions of 3*3*6 mm^3 were machined from the DED manufactured cuboids by electro-discharge machining (EDM) such that the longer (loading) axis was parallel to the build direction (BD). In order to remove the EDM affected surface layer, samples were mechanically ground down to 5 µm grit size. Microstructure analysis was conducted using OM and SEM. The SEM was operated at 20 kV and equipped with an EBSD system. For microstructure analysis, samples were vibration-polished for 3 h with a 0.02 µm colloidal SiO_2 polishing suspension. For OM, samples were additionally etched using a solution of 33 ml ethanol, 8.5 ml H_2O, 50 ml HCl and 8.5 g Cu_2S.

Mechanical tests were carried out using a servo-hydraulic test frame equipped with a digital microscope

and a tele-zoom objective. *In situ* quasi-static uniaxial compression incremental strain tests (IST) were conducted at 100°C in displacement control at a nominal strain rate of $10^{-3}\,s^{-1}$. Heating of the samples was performed by controlled convection furnaces. Temperatures were measured with a thermocouple directly attached to the sample surface. The test temperature was chosen for better comparability with data reported in literature for an ⟨001⟩-oriented single-crystalline reference condition and polycrystalline Co-Ni-Ga structures [8,12,26]. Strains were measured using a high-temperature extensometer with a gauge length of 12 mm directly attached to the grips. For calculation of the nominal strain, the grips were treated as absolutely rigid. Surface images were recorded at the maximum strain as well as after subsequent unloading to −200 N in each increment, employing pre-defined strain intervals of −0.5%. Following mechanical testing, samples were again polished for *post-mortem* EBSD.

Results and discussion

The optical micrograph in Figure 1 reveals crack-free Co-Ni-Ga in the as-built condition fabricated by DED at 500°C. In laser based AM processes, e.g. DED being used in the present study, steep thermal gradients are known to result in high residual stresses [27]. However, it has been shown in literature that elevated base plate temperatures are highly effective to reduce process-induced residual stresses [28]. In addition, in the Co-Ni-Ga system low and intermediate temperatures, i.e. in the range of 350–600°C, promote the precipitation of the ordered $L1_2$ γ'-phase [29,30]. The nanometric precipitates lead to a significant decrease of transformation temperatures (TT), i.e. in contrast to solution-annealed precipitate-free material a precipitation-hardened condition is characterized by TT far below ambient temperature [26,29]. Due to the elevated built temperatures applied in present work, the formation of the γ'-phase is supposed to occur during processing. Thereby, upon final cooling to ambient temperature the thermally induced MT is suppressed (cf. Figure 1) and, concomitantly, stress concentrations at unfavorable GB arrangements are avoided. Finally, in contrast to recent findings for Co-Ni-Ga HT-SMA processed by SLM using lower temperatures [25], material without substantial crack formation has been obtained due to a reduction of internal stresses and a suppression of the thermally induced MT upon cooling.

The optical micrograph and the EBSD analysis in Figures 1 and 2, respectively, highlight the evolution of columnar grains in the as-built material. Due to partial re-melting of the previously deposited material, epitaxial grain growth proceeds across multiple layers parallel

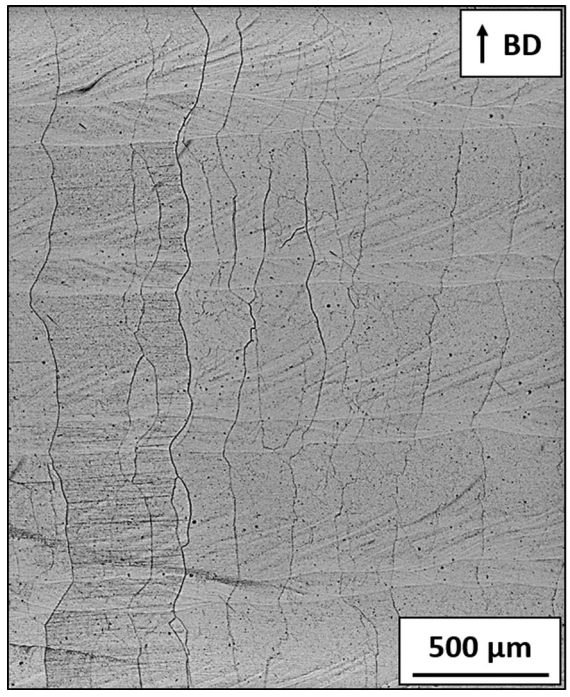

Figure 1. Optical micrograph revealing the microstructure of DED processed Co-Ni-Ga in the as-built condition. BD is vertical.

to BD. The width of the elongated grains is up to 400 µm, whereas their long axes partially exceed the image section of the micrograph (cf. Figure 1) and, thus, are in the millimeter range. Consequently, the columnar grains are characterized by a high aspect ratio (length/width of the grains) $>>1$. In addition, as can be deduced from the inverse pole figure (IPF) mappings (Figure 2a,b) and the IPFs recalculated from EBSD data (Figure 2c,d), these columnar grains feature strong crystallographic texture in near-⟨001⟩ (for better readability ⟨001⟩ in the remainder of the text) and ⟨101⟩ orientation with respect to BD and transverse direction (TD, the direction alongside the scan vector), respectively. In a process parameter window favorable for epitaxial solidification, cubic materials, such as Co-Ni-Ga, show a ⟨001⟩ preferred growth direction along the direction of the maximum thermal gradient [23,24]. As the maximum thermal gradient direction predominately aligns with BD, the evolution of such strong columnar ⟨001⟩ texture alongside BD has been presented and discussed for various cubic materials fabricated by different AM techniques [21,22,24].

The Co-Ni-Ga system is characterized by pronounced tension-compression asymmetry and a strong anisotropy of the MT behavior. According to results obtained by energy minimization theory, maximum transformation strains of 8.6% and −4.8% were found for the ⟨001⟩ crystal direction in tension and compression, respectively [9,14]. In order to evaluate the functional performance under compressive loading, the additively manufactured

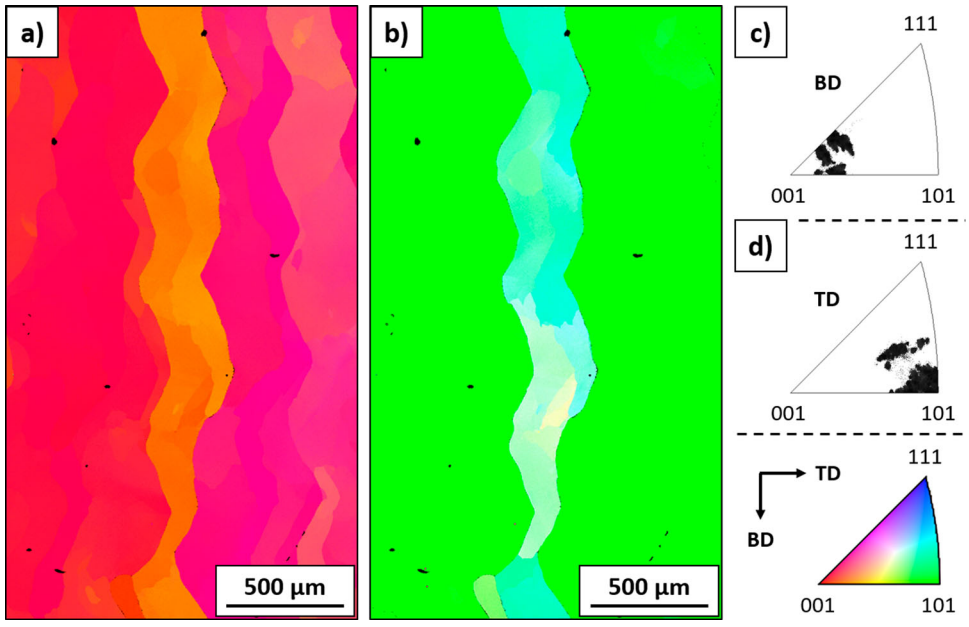

Figure 2. Overview EBSD IPF mappings (a,b) and IPFs (c,d) of DED processed Co-Ni-Ga in the as-built condition. The mappings and IPFs are plotted with respect to BD (a,c) and TD (b,d), respectively. The reference coordinate system and the color-coded standard triangle are shown in the lower right.

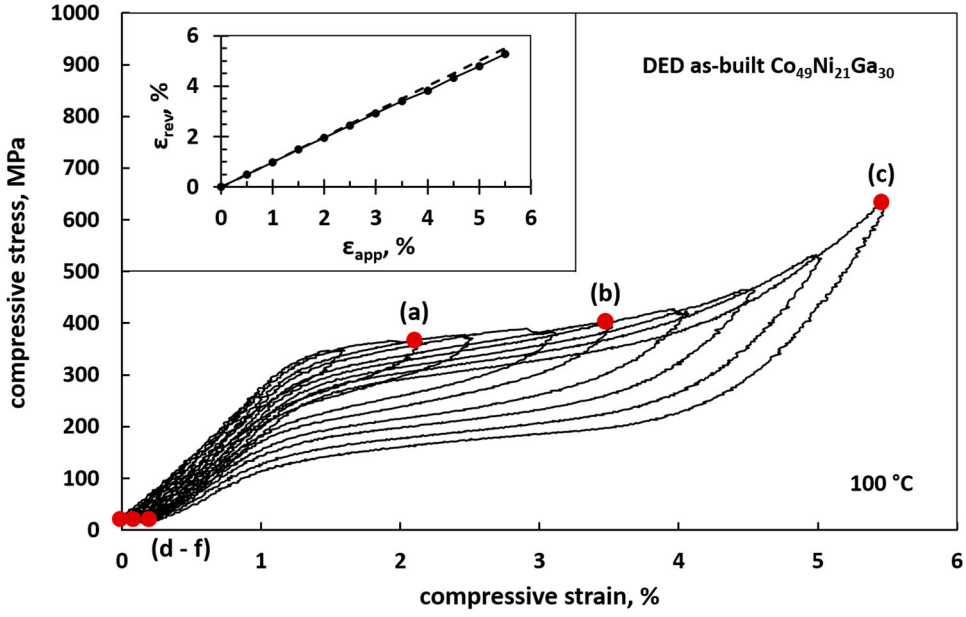

Figure 3. Stress-strain curve at 100°C for DED as-built Co-Ni-Ga under compressive load. Loading direction (LD) is parallel to BD. The red marks (a)–(f) refer to the optical micrographs shown in Figure 4. The relation between reversible ϵ_{rev} and applied strain ϵ_{app} is highlighted in the inset.

material was tested in BD employing *in situ* ISTs at 100°C. A characteristic stress-strain response is shown in Figure 3. The DED Co-Ni-Ga HT-SMA demonstrates a remarkable SE response with an excellent strain recovery of 96% after final unloading from −5.5% strain (cf. inset in Figure 3). The strong crystallographic texture in ⟨001⟩ orientation promotes these superior functional properties, which are competitive to those of ⟨001⟩-oriented Co-Ni-Ga single crystals [26]. However, the additively manufactured material is characterized by an increased stress hysteresis $\Delta\sigma$ and an increased critical stress σ_{cr} for the onset of MT in comparison to the solution-annealed, i.e. precipitate-free, single-crystalline condition [26]. It is important to note that the material in the present study was tested in the as-built condition, i.e. no additional post-process heat treatment has been conducted. It is very likely that the elevated built temperatures result in precipitation of the γ'-phase,

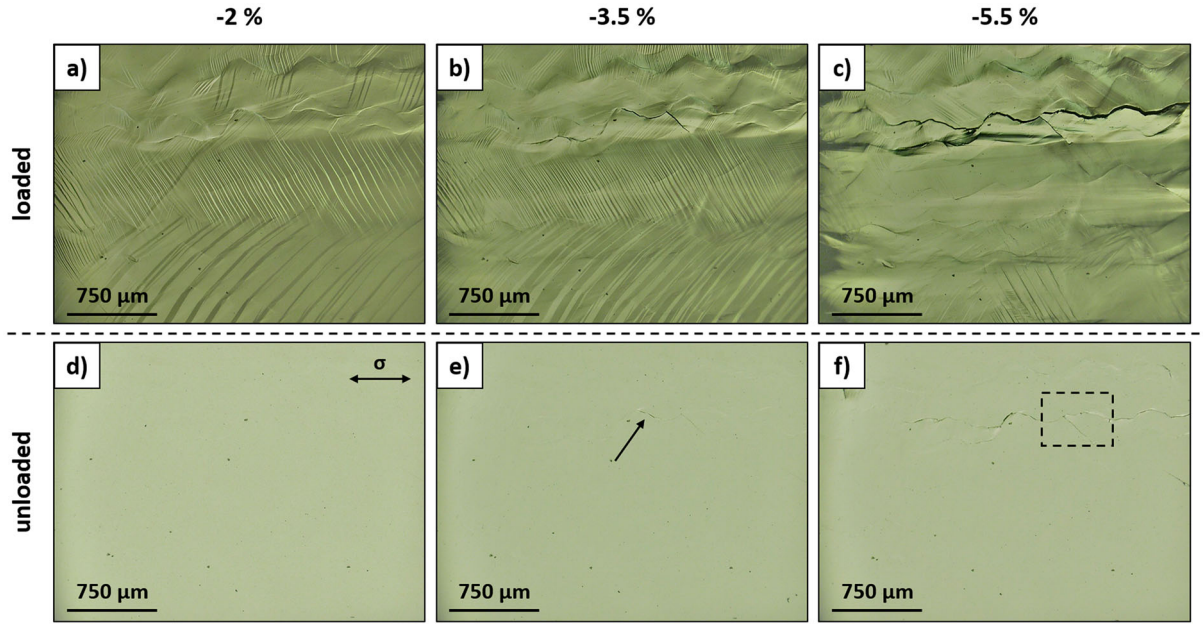

Figure 4. *In situ* analysis under compressive load at 100°C of the as-built Co-Ni-Ga sample shown in Figure 3. Micrographs were recorded under load at strain values of −2%, −3.5% and −5.5% (a–c) and after unloading to −200 N in the same increment (d–f). LD is horizontal (parallel to BD) as indicated in (d). The dashed rectangle in (f) indicates the lateral position of the *post-mortem* SEM analysis (Figure 5).

as has been discussed before. In addition to the TT, this nanometric secondary phase affects the martensitic microstructure [26,29] as well as the functional properties [26,31]. In line with the findings presented in [26,31], the increase of both $\Delta\sigma$ and σ_{cr} compared to precipitate-free single crystals could indicate the existence of fine dispersed γ'-precipitates in the as-built material. Detailed phase analysis of DED processed Co-Ni-Ga will be subject of follow-up studies.

The superior functional performance shown in Figure 3, clearly revealed by the high degree of reversibility, is unusual for SMAs processed by AM. Moghaddam et al. [32] reported very recently for the first time an almost fully reversible SE response with strain recovery of 5.62% (98% recovery ratio) in as-built Ni-Ti (processed by SLM without post-processing). However, in light of the numerous studies focusing on AM of Ni-Ti conducted so far [33], the process window for SLM processing of Ni-Ti seems to be smaller than in case of DED of Co-Ni-Ga. This clearly paves the way for robust direct microstructure design in Co-Ni-Ga by carefully adjusting process parameters, i.e. scan speed, hatch distance, and laser power, as known from structural materials [21,34].

The *in situ* (Figure 4) and *post mortem* (Figure 5) analyses shed light on remaining challenges towards further improvement of the material properties in DED Co-Ni-Ga. Due to the strong crystallographic texture the sample shows a high degree of deformation compatibility upon stress-induced martensitic transformation (SIMT) up to −2% applied strain and, consequently, a fully reversible transformation upon unloading (Figure 4a,d). However, while the deformation comes up to −3.5%, the micrographs in Figure 4b and e illustrate nascent deformation constraints leading to topography changes at specific GBs, which partially remain on the sample surface even after unloading (arrow in Figure 4e). Further deformation to the maximum strain level results in increasing surface topography and, finally, micro-cracking (Figure 4c,f). Considering the cyclic stability, it is expected that the formation of micro-cracks in the very first cycles is of less importance as already reported in [12]. Despite the formation of micro-cracks, a saturation of the formation of residual strain was observed in thermo-mechanically processed Co-Ni-Ga [12]. Investigations on the cyclic stability are in progress and will be reported in future work.

Microstructural features leading to structural degradation upon superelastic loading were investigated by *post mortem* SEM analysis. The EBSD IPF map with superimposed image quality (IQ) in Figure 5 illustrates crack formation, i.e. both inter- and transgranular fracture, in the vicinity of a GB triple junction. Despite the strong texture in the DED processed material, the prevailing triple junction separates grains, which are characterized by considerable different crystallographic orientations, as is shown by the IPF plot highlighting individual labeling of grains in Figure 5. Such triple junctions have been proven to promote high transformation-induced stress concentrations evoking premature fracture and deteriorated functional performance in polycrystalline

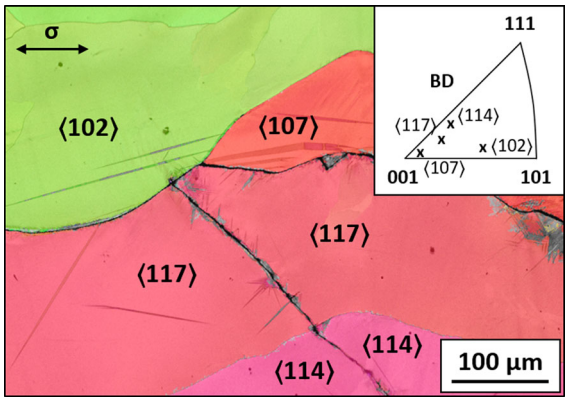

Figure 5. EBSD IPF map with superimposed IQ of the tested as-built Co-Ni-Ga sample shown in Figures 3 and 4. The IPF map is plotted with respect to BD being horizontal and parallel to LD. The inset illustrates the prevailing grain orientations(IPF plot with respect to BD).

structures of relatively brittle and anisotropic SMAs, e.g. Co-Ni-Ga [12,13,16]. Furthermore, martensite plates remain stabilized after final unloading in these particular areas (Figure 5). Both crack formation and stabilized martensite mainly contribute to functional degradation, i.e. accumulation of irreversible strains setting in at an applied strain value of about −3% (cf. inset in Figure 3). In line with the findings on a Cu-based SMA by Liu et al. [17], the key criterion for high-performance polycrystalline Co-Ni-Ga HT-SMAs is the attainment of a highly textured microstructure characterized by the absence of high-angle GBs.

Conclusions

In the present work a crack-free Co-Ni-Ga HT-SMA has been successfully processed by DED at a temperature of 500°C. Due to a distinct coarse columnar grained microstructure and a strong crystallographic texture in near-⟨001⟩ direction alongside BD, excellent SE properties up to −5.5% compressive strain could be revealed for the polycrystalline as-built condition, i.e. DED processed without any post-process heat treatment. In light of envisaged applications and an improved damage tolerance, evaluation of tensile properties as well as further microstructure optimization will be addressed in future studies.

Disclosure statement

No potential conflict of interest was reported by the author(s).

Funding

This work was supported by the Deutsche Forschungsgemeinschaft (DFG) [grant number 398899207].

ORCID

N. Sommer http://orcid.org/0000-0002-5442-8761
M. Vollmer http://orcid.org/0000-0002-8098-8498
P. Krooß http://orcid.org/0000-0001-8310-9631
T. Niendorf http://orcid.org/0000-0003-2622-5817

References

[1] Ma J, Karaman I, Noebe RD. High temperature shape memory alloys. Int Mater Rev. 2013;55:257–315.
[2] Otsuka K, Wayman CM. Shape memory materials. Cambridge: Cambridge University Press; 2002.
[3] Elahinia M, Shayesteh Moghaddam N, Amerinatanzi A, et al. Additive manufacturing of NiTiHf high temperature shape memory alloy. Scr Mater. 2018;145:90–94.
[4] Sehitoglu H, Patriarca L, Wu Y. Shape memory strains and temperatures in the extreme. Curr Opin Solid State Mater Sci. 2017;21:113–120.
[5] Reul A, Lauhoff C, Krooß P, et al. In situ neutron diffraction analyzing stress-induced phase transformation and martensite elasticity in [001]-oriented Co49Ni21Ga30 shape memory alloy single crystals. Shap Mem Superelasticity. 2018;4:61–69.
[6] Oikawa K, Ota T, Gejima F, et al. Phase equilibria and phase transformations in new B2-type ferromagnetic shape memory alloys of Co-Ni-Ga and Co-Ni-Al systems. Mater Trans. 2001;42:2472–2475.
[7] Dadda J, Maier HJ, Karaman I, et al. Pseudoelasticity at elevated temperatures in [001] oriented Co49Ni21Ga30 single crystals under compression. Scr Mater. 2006;55:663–666.
[8] Krooß P, Niendorf T, Kadletz PM, et al. Functional fatigue and tension–compression asymmetry in [001]-oriented Co49Ni21Ga30 high-temperature shape memory alloy single crystals. Shap Mem Superelasticity. 2015;1:6–17.
[9] Monroe JA, Karaman I, Karaca HE, et al. High-temperature superelasticity and competing microstructural mechanisms in Co49Ni21Ga30 shape memory alloy single crystals under tension. Scr Mater. 2010;62:368–371.
[10] Niendorf T, Krooß P, Somsen C, et al. Martensite aging – avenue to new high temperature shape memory alloys. Acta Mater. 2015;89:298–304.
[11] Lauhoff C, Krooß P, Langenkämper D, et al. Martensite aging in ⟨001⟩ oriented Co49Ni21Ga30 single crystals in tension. Funct Mater Lett. 2018;11:1850024.
[12] Vollmer M, Krooß P, Segel C, et al. Damage evolution in pseudoelastic polycrystalline Co–Ni–Ga high-temperature shape memory alloys. J Alloys Compd. 2015;633:288–295.
[13] Lauhoff C, Vollmer M, Krooß P, et al. Pathways towards grain boundary engineering for improved structural performance in polycrystalline Co–Ni–Ga shape memory alloys. Shap Mem Superelasticity. 2019;5:73–83.
[14] Dadda J, Maier HJ, Niklasch D, et al. Pseudoelasticity and cyclic stability in Co49Ni21Ga30 shape-memory alloy single crystals at ambient temperature. Metall and Mat Trans A. 2008;39:2026–2039.
[15] Ueland SM, Chen Y, Schuh CA. Oligocrystalline shape memory alloys. Adv Funct Mater. 2012;22:2094–2099.

[16] Ueland SM, Schuh CA. Grain boundary and triple junction constraints during martensitic transformation in shape memory alloys. J Appl Phys. 2013;114:53503.
[17] Liu J-L, Huang H-Y, Xie J-X. The roles of grain orientation and grain boundary characteristics in the enhanced superelasticity of Cu71.8Al17.8Mn10.4 shape memory alloys. Mater Des. 2014;64:427–433.
[18] Sutou Y, Omori T, Kainuma R, et al. Grain size dependence of pseudoelasticity in polycrystalline Cu–Al–Mn-based shape memory sheets. Acta Mater. 2013;61:3842–3850.
[19] Karsten E, Gerstein G, Golovko O, et al. Tailoring the microstructure in polycrystalline Co–Ni–Ga high-temperature shape memory alloys by hot extrusion. Shap Mem Superelasticity. 2019;5:84–94.
[20] Niendorf T, Lauhoff C, Karsten E, et al. Direct microstructure design by hot extrusion – high-temperature shape memory alloys with bamboo-like microstructure. Scr Mater. 2019;162:127–131.
[21] Niendorf T, Leuders S, Riemer A, et al. Functionally graded alloys obtained by additive manufacturing. Adv Eng Mater. 2014;16:857–861.
[22] Todaro CJ, Easton MA, Qiu D, et al. Grain structure control during metal 3D printing by high-intensity ultrasound. Nat Commun. 2020;11:142.
[23] Glicksman ME. Principles of solidification: an introduction to modern casting and crystal growth concepts. New York: Springer; op. 2011.
[24] Thijs L, Montero Sistiaga ML, Wauthle R, et al. Strong morphological and crystallographic texture and resulting yield strength anisotropy in selective laser melted tantalum. Acta Mater. 2013;61:4657–4668.
[25] Lauhoff C, Fischer A, Sobrero C, et al. Additive manufacturing of Co-Ni-Ga high-temperature shape memory alloy: processability and phase transformation behavior. Metall and Mat Trans A. 2020;50:511.
[26] Lauhoff C, Reul A, Langenkämper D, et al. Effect of nanometric γ'-particles on the stress-induced martensitic transformation in ⟨001⟩-oriented Co49Ni21Ga30 shape memory alloy single crystals. Scr Mater. 2019;168:42–46.
[27] Mercelis P, Kruth J-P. Residual stresses in selective laser sintering and selective laser melting. Rapid Prototyp J. 2006;12:254–265.
[28] Breidenstein B, Brenne F, Wu L, et al. Effect of post-process machining on surface properties of additively manufactured H13 tool steel. HTM. 2018;73:173–186.
[29] Kireeva IV, Pons J, Picornell C, et al. Influence of γ' nanometric particles on martensitic transformation and twinning structure of L10 martensite in Co–Ni–Ga ferromagnetic shape memory single crystals. Intermetallics. 2013;35:60–66.
[30] Chumlyakov YI, Kireeva IV, Panchenko EY, et al. High-temperature superelasticity in CoNiGa, CoNiAl, NiFeGa, and TiNi monocrystals. Russ Phys J. 2008;51:1016–1036.
[31] Kireeva IV, Picornell C, Pons J, et al. Effect of oriented γ' precipitates on shape memory effect and superelasticity in Co–Ni–Ga single crystals. Acta Mater. 2014;68:127–139.
[32] Shayesteh Moghaddam N, Saedi S, Amerinatanzi A, et al. Achieving superelasticity in additively manufactured NiTi in compression without post-process heat treatment. Sci Rep. 2019;9:41.
[33] Elahinia M, Shayesteh Moghaddam N, Taheri Andani M, et al. Fabrication of NiTi through additive manufacturing: a review. Prog Mater Sci. 2016;83:630–663.
[34] Brenne F, Niendorf T. Damage tolerant design by microstructural gradation – influence of processing parameters and build orientation on crack growth within additively processed 316L. Mater Sci Eng A. 2019;764:138186.